Inorg. Chem. **2008**, *47*, 9979−9986

Anionic Layered Networks Reconstructed from $[Cd(SCN)_3]_\infty^-$ Chains in Pseudo One-Dimensional Conducting Salts of Halogenated Tetrathiafulvalenes

Marc Fourmigué*,† and Pascale Auban-Senzier‡

Sciences Chimiques de Rennes, Université Rennes 1, UMR CNRS 6226, Campus de Beaulieu, 35042 Rennes, France, and Laboratoire de Physique des Solides, Université Paris-Sud, UMR CNRS 8502, Bât. 510, 91405 Orsay, France

Received June 30, 2008

The electrocrystallization of diiodo- and dibromo-ethylenedithiotetrathiafuvalene (EDT-TTFI_2 and EDT-TTFBr_2) in the presence of the polymeric 1D $[Et_4N][Cd(SCN)_3]$ as an electrolyte affords two different salts, formulated as $[EDT\text{-}TTF\text{-}I_2]_4[Cd_3(NCS)_8]\cdot CH_3CN\cdot H_2O$ (**1**) and $[EDT\text{-}TTF\text{-}Br_2]_{10}[Cd_5(SCN)_{14}]\cdot 2TCE$ (**2**), characterized by a two-dimensional segregation of the partially oxidized donor molecules and the polymeric anionic network incorporating embedded solvent molecules. Both salts exhibit a partial charge transfer, that is, $\rho = 0.5$ in **1** and an unconventional $\rho = 0.4$ in **2**. They behave as semiconductors with $\sigma_{RT} = 0.67$ and 33 S cm^{-1} and activation energies of 330 and 370 K for **1** and **2**, respectively. Compared with a 1:3 Cd/SCN ratio of the starting electrolyte, the reconstructed, thiocyanate (SCN)-deficient motifs $[Cd_3(NCS)_8]^{2-}$ and $[Cd_5(SCN)_{14}]^{4-}$ organize into layered hollow structures with cavities filled by solvent molecules, halogen-bonded to the halogenated TTF molecules, through a $C_{TTF}-I\cdots N\equiv C-CH_3$ interaction in **1**, through a type II $C_{TTF}-Br\cdots Cl-C_{TCE}$ halogen/halogen interaction in **2**. Band structure and Fermi surface calculations for the two salts indicate a two-dimensional character, while the semiconducting properties of the salts are attributed to an efficient nesting of the hidden 1D Fermi surfaces.

Introduction

The electronic properties of molecular conductors are intimately dependent on the precise solid-state arrangement of the partially oxidized donor molecules in the crystalline solid state, which controls indeed the details of the band structure of the materials. For a given donor molecule, several strategies have been envisioned to influence this solid-state organization during the electro-crystallization experiments, by modifying the nature, shape, and charge of the counterions, but also by introducing weak intermolecular interactions at the organic/inorganic interface. For example, tetrathiafulvalenes (TTFs) have been functionalized with hydrogen-bond donor groups such as carboxylic[1] or phosphonic acids,[2] amides,[3] or thioamides,[4] in order to induce specific hydrogen bonds with the anionic network acting as hydrogen-bond acceptor.[5] Similarly, halogen bonding, which describes an interaction between an organic halide and a Lewis base,[6] has been also investigated in the realm of conducting materials.[5,7] The oxidation of halogenated TTFs—essentially iodo and bromo derivatives—enhances the partial positive charge on the halogen atom, which then exhibits a strong tendency to interact with counterions, which act as a Lewis base to give structural motifs such as $TTF-I\cdots Br^-$ with halide anions,[8] $TTF-I\cdots I_3^-$ with polyhaloanions,[9] $TTF-I\cdots[X_nM]^{-m}$ with polyhalometalates,[10,11] or $TTF-I\cdots[(NC)_nM]^{-m}$ with cyanometallates[12] or anionic nitriles.[13] Electrocrystallization of iodo-TTFs with the complex $[Cr(isoq)_2(NCS)_4]^-$ anion also showed that halogen bonding

* Author to whom correspondence should be addressed. E-mail: marc.fourmigue@univ-rennes1.fr.
† Université Rennes 1.
‡ Université Paris-Sud.

(1) (a) Mézière, C.; Fourmigué, M.; Fabre, J.-M. C. R. *Acad. Sci. Paris, IIc* **2000**, *3*, 387. (b) Heuzé, K.; Fourmigué, M.; Batail, P. *J. Mater. Chem.* **1999**, *9*, 2373. (c) Dolbecq, A.; Fourmigué, M.; Batail, P. *Bull. Soc. Chim. Fr.* **1996**, *133*, 83.
(2) Dolbecq, A.; Fourmigué, M.; Krebs, F. C.; Batail, P.; Canadell, E.; Clérac, R.; Coulon, C. *Chem.—Eur. J.* **1996**, *2*, 1275.
(3) (a) Ono, G.; Izuoka, A.; Sugawara, T.; Sugawara, Y. *J. Mater. Chem.* **1998**, *8*, 1703. (b) Heuzé, K.; Fourmigué, M.; Batail, P. *J. Mater. Chem.* **1999**, *9*, 2373. (c) Heuzé, K.; Fourmigué, M.; Batail, P.; Canadell, E.; Auban-Senzier, P. *Chem.—Eur. J.* **1999**, *5*, 2971. (d) Heuzé, K.; Mézière, C.; Fourmigué, M.; Batail, P.; Coulon, C.; Canadell, E.; Auban-Senzier, P.; Jérome, D. *Chem. Mater.* **2000**, *12*, 1898.

10.1021/ic801207v CCC: $40.75
Published on Web 10/08/2008

could involve the sulfur atom of the thiocyanate anion.[14] Recently, we investigated the ability of such partially oxidized halogenated TTFs to interact not only with isolated counterions but also with extended polymeric anionic arrays. For example, the electrocrystallization of EDT-TTF-I_2 in the presence of a mixture of PbI_2 and NaI in CH_3CN afforded a layered material formulated as β-(EDT-TTF-I_2)$_2^{+\bullet}$[$(Pb_{5/6}\square_{1/6}I_2)_{1/3}^-$]$_3$, where the anionic charge of the PbI_2 layer is obtained through Pb^{2+} lacunas (□).[15] On the other hand, the use of the polymeric $(Bu^nNH_3)_2PbI_4$ with NaI or KI in CH_3CN afforded a salt formulated as (EDT-TTFI_2)$_2PbI_3\cdot H_2O$, characterized by one-dimensional ribbons of face-sharing $[PbI_{6/2}^-]_\infty$ octahedra.[16] In both compounds, C−I···I−Pb halogen-bonding interactions were identified at the organic/inorganic interface.

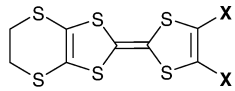

Combining the several approaches described above, we were particularly attracted by the salts of cadmium thiocyanate formulated as $[Cd_m(SCN)_n]^{2m-n}$, which were described to crystallize into a wide variety of polymeric arrays,[17] due to the comparable ability of both the nitrogen and the sulfur atom of the thiocyanate anion to coordinate the cationic Cd^{2+} center. Indeed, the ambidentate nature of the thiocyanate anion allows for a variety of bridging modes, among which the most common are collected in Scheme 1. On the basis of the hard−soft acid−base concept developed by Pearson, Basolo, and Burmeister,[18] the first transition metals as well as the lanthanides and actinides exhibit only N coordination. The first half of the second and third transition series tends to N coordination, whereas at Rh(III) and Ir(III), there is a switch to S coordination. This brings an interesting situation for the Zn−Cd−Hg triad and particularly the Cd(II), which becomes "schizophrenic",[17] and exhibits both (S and N) coordination and an variety of coordination numbers. A good solubility in organic solvents is required to be able to use such $[Cd_m(SCN)_n]^{2m-n}$ cadmium thiocyanate salts as electrolytes in electrocrystallization experiments. Therefore, we turn our attention toward the tetraalkyl ammonium salts of the anionic $[Cd(SCN)_3]^-$, which are described to crystallize into infinite chains, as shown in Scheme 1b.[19] This one-dimensional motif appears as a recurrent feature in many other salts of $[Cd(SCN)_3]^-$with ammonium as well as metal crown-ether cations,[20,21] while one example of a three-dimensional organization was recently reported for the $[Cd(SCN)_3]^-$ system, based on the templating effect of the cationic counterion.[22]

Scheme 1. (a) The Most Usual Bridging Mode of the Thiocyanate Ligand and (b) the 1D Polymeric Motif Frequently Adopted by $[Cd(SCN)_3]^-$

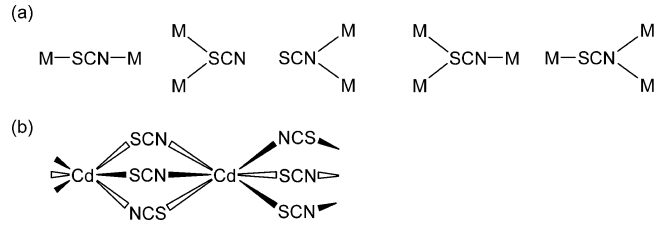

Considering the apparent robustness of these $[Cd(SCN)_3]^-$ chains, we therefore decided to use them as electrolytes in electrocrystallization experiments with TTF derivatives, allowing us to concentrate on halogenated TTFs in order to evaluate the possibility for halogen-bonding interactions with the thiocyanate anions, at the organic/inorganic interface. We describe here the salts obtained upon electro-crystallization of diiodo- and dibromo-ethylenedithiotetrathiafuvalene (EDT-TTFI_2 and EDT-TTFBr_2) in the presence of the polymeric $[Et_4N][Cd(SCN)_3]$ as an electrolyte. Original two-dimensional honeycomb anionic networks incorporating solvent

(4) (a) Moore, A. J.; Bryce, M. R.; Batsanov, A. S.; Heaton, J. N.; Lehmann, C. W.; Howard, J. A. K.; Robertson, N.; Underhill, A. E.; Perepichka, I. F. *J. Mater. Chem.* **1998**, *8*, 1541. (b) Batsanov, A. S.; Bryce, M. R.; Cooke, G.; Heaton, J. N.; Howard, J. A. K. *J. Chem. Soc., Chem. Commun.* **1993**, 1701. (c) Batsanov, A. S.; Bryce, M. R.; Cooke, G.; Dhindsa, A. S.; Heaton, J. N.; Howard, J. A. K.; Moore, A. J.; Petty, M. C. *Chem. Mater.* **1994**, *6*, 1419.
(5) Fourmigué, M.; Batail, P. *Chem. Rev.* **2004**, *104*, 5379.
(6) Metrangolo, P.; Resnati, G. *Struct. Bonding (Berlin)* **2008**, *126*.
(7) Fourmigué, M. *Struct. Bonding (Berlin)* **2008**, *126*, 181.
(8) (a) Imakubo, T.; Sawa, H.; Kato, R. *Synth. Met.* **1995**, *73*, 117. (b) Imakubo, T.; Shirahata, T.; Hervé, K.; Ouahab, L. *J. Mater. Chem.* **2006**, *16*, 162. (c) Gompper, R.; Hock, J.; Pollborn, K.; Dormann, E.; Winter, H. *Adv. Mater.* **1995**, *7*, 41.
(9) (a) Iyoda, M.; Kuwatani, Y.; Hara, K.; Ogura, E.; Suzuki, H.; Ito, H.; Mori, T. *Chem. Lett.* **1997**, 599. (b) Domercq, B.; Devic, T.; Fourmigué, M.; Auban-Senzier, P.; Canadell, E. *J. Mater. Chem.* **2001**, *11*, 1570.
(10) (a) Miyazaki, A.; Enomoto, K.; Okabe, K.; Yamazaki, H.; Nishijo, J.; Enoki, T.; Ogura, E.; Ugawa, K.; Kuwatani, Y.; Iyoda, M. *J. Solid State Chem.* **2002**, *168*, 547. (b) Nishijo, J.; Miyazaki, A.; Enoki, T.; Watanabe, R.; Kuwatani, Y.; Iyoda, M. *Inorg. Chem.* **2005**, *44*, 2493. (c) Shirahata, T.; Kibune, M.; Maesato, M.; Kawashima, T.; Saito, G.; Imakubo, T. *J. Mater. Chem.* **2006**, *16*, 3381.
(11) Alberola, A.; Fourmigué, M.; Gómez-García, C. J.; Llusar, R.; Triguero, S. *New J. Chem.* **2008**, *32*, 1103.
(12) (a) Ranganathan, A.; El-Ghayoury, A.; Mézière, C.; Harté, E.; Clérac, R.; Batail, P. *Chem. Commun.* **2006**, 2878. (b) Ouahab, L.; Setifi, F.; Golhen, S.; Imakubo, T.; Lescouezec, R.; Lloret, F.; Julve, M.; Swietlik, R. *C. R. Chim.* **2005**, *8*, 1286.
(13) (a) Devic, T.; Domercq, B.; Auban-Senzier, P.; Molinié, P.; Fourmigué, M. *Eur. J. Inorg. Chem.* **2002**, 2844. (b) Batsanov, A. S.; Moore, A. J.; Robertson, N.; Gree, A.; Bryce, M. R.; Howard, J. A. K.; Underhill, A. E. *J. Mater. Chem.* **1997**, *7*, 387. (c) Nishijo, J.; Ogura, E.; Yamaura, J.; Miyazaki, A.; Enoki, T.; Takano, T.; Kuwatani, Y.; Iyoda, M. *Solid State Commun.* **2000**, *116*, 661.
(14) Hervé, K.; Cador, O.; Golhen, S.; Costuas, K.; Halet, J.-F.; Shirahata, T.; Muto, T.; Imakubo, T.; Miyazaki, A.; Ouahab, L. *Chem. Mater.* **2006**, *18*, 790.
(15) Devic, T.; Evain, M.; Moëlo, Y.; Canadell, E.; Auban-Senzier, P.; Fourmigué, M.; Batail, P. *J. Am. Chem. Soc.* **2003**, *125*, 3295.
(16) Devic, T.; Canadell, E.; Auban-Senzier, P.; Batail, P. *J. Mater. Chem.* **2004**, *14*, 135.
(17) Zhang, H.; Wang, X.; Zhang, K.; Teo, B. K. *Coord. Chem. Rev.* **1999**, *183*, 157.
(18) (a) Pearson, R. G. *J. Am. Chem. Soc.* **1963**, *85*, 3533. (b) Pearson, R. G. *Adv. Inorg. Chem. Radiochem.* **1966**, *8*, 177. (c) Basolo, F. *Coord. Chem. Rev.* **1968**, *3*, 213. (d) Burmeister, J. L. *Chem. Rev.* **1968**, *3*, 225.
(19) Taniguchi, M.; Ouchi, A. *Bull. Chem. Soc. Jpn.* **1989**, *62*, 424.
(20) (a) Zhang, H.; Wang, X.; Zelmon, D. E.; Teo, B. K. *Inorg. Chem.* **2001**, *40*, 1501. (b) Zhang, H.; Zelmon, D. E.; Price, G. E.; Teo, B. K. *Inorg. Chem.* **2000**, *39*, 1868. (c) Zhang, H.; Wang, X.; Teo, B. K. *J. Am. Chem. Soc.* **1996**, *118*, 11813.
(21) (a) Harrington, J. M.; Jones, S. B.; White, P. H.; Hancock, R. D. *Inorg. Chem.* **2004**, *43*, 4456. (b) Bala, R.; Kennedy, A. R.; Saneja, K.; Sharma, R. P. *Acta Crystallogr.* **2006**, *E62*, m1630. (c) Russo, L.; Sharma, R. P.; Sharma, S.; Sharmaz, R.; Rissanen, K. *Acta Crystallogr.* **2006**, *E62*, m2011.
(22) Lai, L.-L.; Wu, C.-H.; Lu, K.-L.; Wen, Y.-S.; Liu, Y.-H.; Wang, Y.; Cheng, K.-L.; Soldatov, D. V.; Yu, Z.; Yu, K. *CystEngComm* **2007**, *9*, 345.

Table 1. Crystallographic Data[a]

compound	**1**	**2**
formula	$C_{22}H_{12}Cd_{1.50}I_4N_5OS_{16}$	$C_{48}H_{21.50}Br_{10}Cd_{2.50}Cl_{1.50}N_7S_{37}$
fw ($g \cdot mol^{-1}$)	1551.53	3015.72
cryst color	black	black
cryst shape	prism	prism
cryst size (mm)	0.5 × 0.3 × 0.25	0.35 × 0.13 × 0.03
cryst syst	triclinic	triclinic
space group	$P\bar{1}$	$P\bar{1}$
T (K)	293(2)	293(2)
a (Å)	8.79570(10)	14.3707(4)
b (Å)	12.9571(2)	18.0459(5)
c (Å)	19.6473(4)	19.4342(4)
α (deg)	104.318(8)	86.7917(17)
β (deg)	95.7570(10)	72.7663(15)
γ (deg)	95.48590(10)	69.5448(13)
V (Å^3)	2141.74(6)	4503.7(2)
Z	2	2
D_{calcd} ($g \cdot cm^{-3}$)	2.406	2.224
μ (mm^{-1})	4.444	5.966
total reflns	37828	62068
absorption correction	multiscan	multiscan
T_{min}, T_{max}	0.1913, 0.285	0.3415, 0.6281
unique reflns (R_{int})	9766 (0.0819)	20582 (0.0954)
unique reflns ($I > 2\sigma(I)$)	8004	12515
R_1, wR_2 ($I > 2\sigma(I)$)	0.0398, 0.1013	0.0577, 0.1448
R_1, wR_2 (all data)	0.051, 0.1103	0.1056, 0.1723
goodness-of-fit	1.088	1.014
residual dens (e^-Å^{-3})	+2.31, −1.39	+2.104, −1.009

[a] $R_1 = \sum||F_o| - |F_c||/\sum|F_o|$. $wR_2 = [\sum w(F_o^2 - F_c^2)^2/\sum wF_o^4]^{1/2}$.

molecules were stabilized, while the organic slabs adopt electronic structures characteristic of one-dimensional conductors with unusual band filling.

Experimental Section

Electro-Crystallization Experiments. The donor molecules[9b] and the electrolyte[19] were synthesized as previously described and recrystallized twice before use. Both salts were prepared starting from 10 mg of the donor molecule and 100 mg of $Et_4N[Cd(SCN)_3]$ in a 1:1 mixture of acetonitrile and 1,1,2-trichloroethane. The cells were thermostatted at 30° and the electro-crystallizations performed with a current of 0.5 μA with Pt electrodes (length 1.5 cm, diameter 1 mm) for 2 weeks.

X-Ray Diffraction Studies. Single crystals were mounted on the top of a thin glass fiber. Data were collected on a Nonius KappaCCD Diffractometer at room temperature with graphite-monochromated Mo Kα radiation ($\lambda = 0.71073$ Å). Structures were solved by direct methods (SHELXS-97) and refined (SHELXL-97)[23] by full-matrix least-squares methods, as implemented in the WinGX software package.[24] Absorption corrections were applied. Hydrogen atoms were introduced at calculated positions (riding model), included in structure factor calculations, and not refined. Crystallographic data of both salts are summarized in Table 1. The carbon atoms of the TCE molecule in **2** (C9 and C10) as well as the ethylene group in the disordered EDT-TTFBr_2 molecule (molecule C) were refined isotropically.

Band Structure Calculations. The tight-binding band structure calculations and $\beta_{HOMO-HOMO}$ interaction energies were based upon the effective one-electron Hamiltonian of the extended Hückel method,[25] as implemented in the Caesar 1.0 chain of programs.[26] The off-diagonal matrix elements of the Hamiltonian were calculated according to the modified Wolfsberg−Helmholz formula.[27] All valence electrons were explicitly taken into account in the calculations, and the basis set consisted of double-ζ Slater-type orbitals for C, S, Br, and I and single-ζ Slater-type orbitals for H. The exponents, contraction coefficients, and atomic parameters for C, S, Br, I, and H were taken from previous work.[9b]

Results and Discussion

The one-dimensional polymeric cadmium thiocyanate complex anion $[Cd(SCN)_3]_\infty^-$ was prepared as previously described from Et_4NCl, $CdSO_4$, and KSCN.[19] $[Et_4N][Cd(SCN)_3]$ was isolated as a colorless crystalline solid, soluble in CH_3CN. Electro-crystallizations of EDT-TTF-I_2 and EDT-TTF-Br_2 were performed in the presence of $[Et_4N][Cd(SCN)_3]$ in a 1:1 acetonitrile/1,1,2-trichloroethane (TCE) mixture at 30 °C. Black parallelepipedic crystals were collected on the anode. Both salts crystallize in the triclinic system, space group $P\bar{1}$, but are not isostructural. Indeed, with EDT-TTF-I_2, X-ray crystal structure resolution afforded the $[EDT\text{-}TTF\text{-}I_2]_4[Cd_3(NCS)_8] \cdot CH_3CN \cdot H_2O$ (**1**) formulation with acetonitrile and water inclusion, while another stoichiometry, combined with TCE inclusion, was indeed obtained with EDT-TTF-Br_2, which is thus formulated as $[EDT\text{-}TTF\text{-}Br_2]_{10}[Cd_5(SCN)_{14}] \cdot 2TCE$ (**2**). We already note that these formulations also correspond to different oxidation degrees (ρ) for the donor molecules, $\rho = +0.5$ in **1** for EDT-TTF-I_2 with the dianionic $[Cd_3(SCN)_8]^{2-}$ species, but $\rho = +0.4$ in **2** with EDT-TTF-Br_2 and the tetraanionic $[Cd_5(SCN)_{14}]^{4-}$ species. The latter represents a rare oxidation state in these materials, which very often stabilize in the $\rho = +0.5$ state.[28] Both salts exhibit a temperature dependence of the conductivity characteristic of semiconductors, with $\sigma_{RT} = 0.67$ and 33 S cm^{-1} and activation energies of 330 and 370 K for **1** and **2**, respectively, with a 50 times higher RT conductivity for compound **2**, characterized with this unconventional oxidation state ($\rho = +0.4$).

The Complex Lacunary Anionic Layers. In **1**, the asymmetric unit is composed of two EDT-TTF-I_2 molecules in a general position in the unit cell (noted A and B in the following), one Cd^{2+} cation on an inversion center (Cd1), and one Cd^{2+} cation in general position (Cd2), together with eight SCN^- anions coordinated to the cadmium cations. A view of the unit cell of the EDT-TTF-I_2 salt **1** (Figure 2) shows the two-dimensional segregation of the cationic organic and anionic inorganic parts, while Figure 3 gives details of the complex organization adopted by the inorganic layer.

Two halogen bonding interactions are identified at the organic/inorganic interface that involve one iodine atom of each of the crystallographically independent EDT-TTFI_2 molecules, that is, I1A and I1B. As shown in Figure 3, the iodine atom I1A is bonded to the nitrogen atom of an acetonitrile molecule embedded in the inorganic layer (vide

(23) Sheldrick, G. M. *SHELX97*, release 97-2; Bruker AXS: Madison, WI, 1998.
(24) Farrugia, L. J. *J. Appl. Crystallogr.* **1999**, *32*, 837.
(25) Whangbo, M.-H.; Hoffmann, H. *J. Am. Chem. Soc.* **1978**, *100*, 6093.
(26) Ren, J.; Liang, W.; Whangbo, M.-H. *Crystal and Electronic Structure Analysis Using CAESAR*; PrimeColor Software Inc.: Cary, North Carolina, 1998.
(27) Ammeter, J.; Bürgi, H.-B.; Thibeault, J.; Hoffmann, R. *J. Am. Chem. Soc.* **1978**, *100*, 3686.
(28) For a review on unusual oxidation states, see: (a) Mori, T. *Chem. Rev.* **2004**, *104*, 4947.

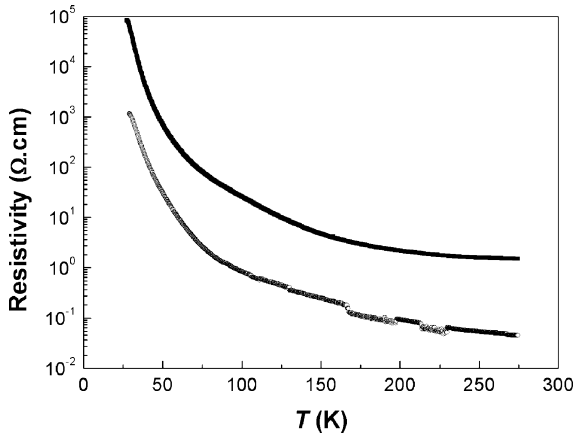

Figure 1. Temperature dependence of the resistivity of **1** (●) and **2** (○).

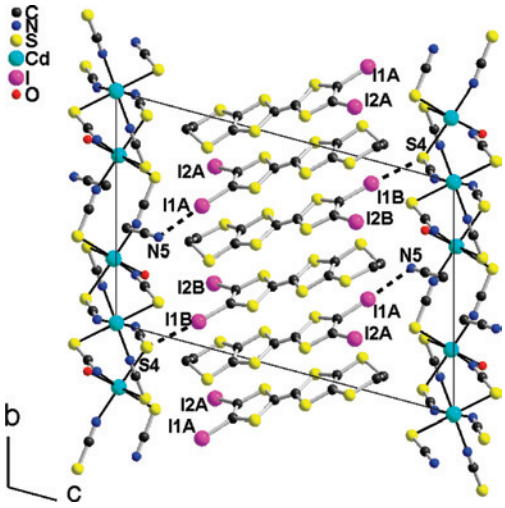

Figure 2. Projection view (along *a*) of the unit cell of $[EDT\text{-}TTF\text{-}I_2]_4[Cd_3(NCS)_8 \cdot H_2O] \cdot 2CH_3CN$ (**1**). Note the I1A···N5 halogen bond interaction (black dotted lines, see text).

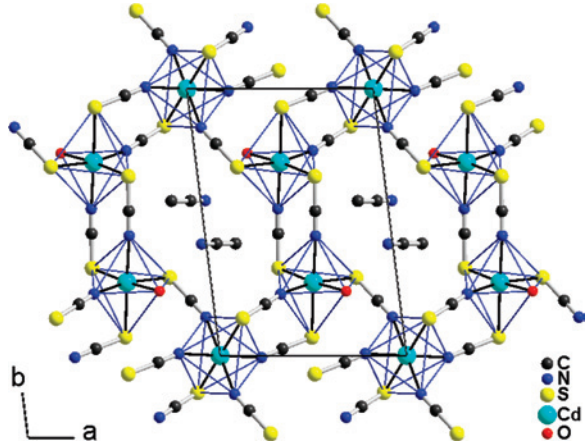

Figure 3. Detail of the structure of the polymeric $[Cd_3(NCS)_8 \cdot 2H_2O]^{2-} \cdot 2CH_3CN$ anionic network in **1**, showing the octahedral coordination of the Cd^{2+} cations and the acetonitrile molecules embedded in the holes of the anionic polymeric lattice.

infra). Structural characteristics for this interaction, that is, I···N, 3.023(16) Å; C−I···N, 177.2(2)°; I···N≡C, 109.9(4)°; point to a linear and rather strong interaction, if we compare the I···N contact distance with the van der Waals contact distance (3.68 Å) or the contact distance predicted from the

Scheme 2. (Left) Definition of the r_{min} and r_{max} and (Right) the Two Different Types of Halogen Interactions, as Described in ref 30a

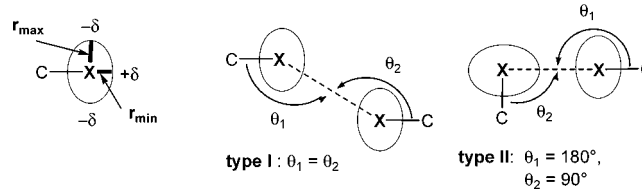

anisotropic model ($r_{minI} + r_N = 3.36$ Å).[29] Similarly (Figure 2), the iodine atom I1B is linked to a thiocyanate sulfur atom (S4) with favorable structural features, that is, I···S, 3.248(16) Å; C−I···S, 174.11(11)°; and I···S−C, 87.92(14)°. Again, the I···S distance is strongly linear and very short, when compared with the van der Waals contact distance (3.72 Å) or with the contact distance predicted from the anisotropic model ($r_{minI} + r_{maxS} = 3.79$ Å),[29] while the C−I···S and I···S−C angles are close to 180 and 90°, a typical feature of the so-called type II halogen bonding interaction, as described by Desiraju and Parthasarathy (Scheme 2).[30]

As shown in Figure 3, we also observe that each cadmium atom is hexacoordinated, lying at the center of a distorted octahedron, with Cd1 coordinated by four nitrogen atoms and two sulfur atoms while Cd2 is coordinated by three sulfur, two nitrogen, and one oxygen atom, the latter belonging to a water molecule. In this structure, each thiocyanate is therefore involved in coordination both through its nitrogen and through its sulfur ends, affording a rigid, two-dimensional porous network, where the empty spaces are filled by two acetonitrile molecules related by an inversion center. These two solvent molecules do not just fill the holes but are anchored to the organic slabs as the nitrogen atom of the acetonitrile molecules is indeed engaged in a halogen bond with the iodine atom of an organic donor (vide supra).

As mentioned above, the formulation of **2**, that is, $[EDT\text{-}TTF\text{-}Br_2]_{10}[Cd_5(SCN)_{14}] \cdot 2TCE$, lets us infer even more complex anionic inorganic and cationic organic structural organizations, besides the recurrent organic/inorganic segregation shown in Figure 4.

Of particular note already is the halogen-bonding interactions, which settle between the bromine atoms of two $EDT\text{-}TTFBr_2$ molecules (molecules B and E) and, respectively, the sulfur atoms of two SCN anions (with molecule B) and the chlorine atom of the included TCE molecule (dotted lines in Figure 4). Their geometrical characteristics are collected in Table 2 and point unambiguously to type II halogen-bonding interactions (Scheme 2) characterized indeed by short Br···(Cl/S) distances and C−Br···(Cl/S) and Br···(Cl/S)−C angles close to 180 and 90°, respectively.[29]

The anionic layer in **2** (Figure 5) is now formed from three crystallographically independent Cd^{2+} cations, one on an inversion center (Cd1) and two in general positions (Cd2 and Cd3), coordinated by seven different thiocyanate am-

(29) Nyburg, S. C.; Faerman, C. H. *Acta Crystallogr.* **1985**, *B41*, 274.
(30) (a) Desiraju, G. R.; Parthasarathy, R. *J. Am. Chem. Soc.* **1989**, *111*, 8725. (b) Price, S. L.; Stone, A. J.; Lucas, J.; Rowland, R. S.; Thornley, A. E. *J. Am. Chem. Soc.* **1994**, *116*, 4910.

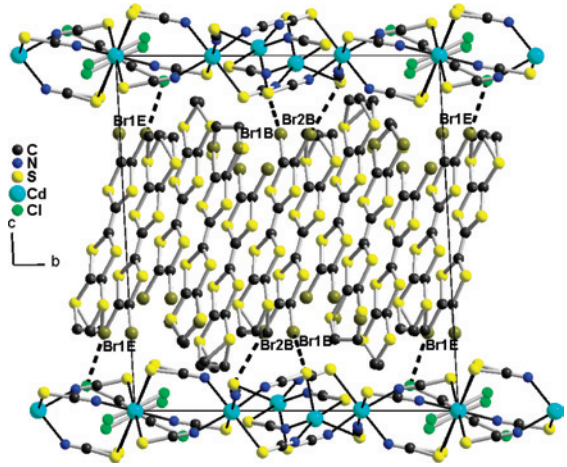

Figure 4. Projection view along *a* of the unit cell of **2**. The dotted lines indicate the halogen bonding interactions between the bromine atoms of the EDT-TTFBr$_2$ molecules and the chlorine or sulfur atoms of the anionic layer (see text).

Table 2. Geometrical Characteristics of the Halogen Bonding Interactions Identified in **2**[a]

interaction	Br···(Cl/S) (Å)	vdW dist. (Å)	anis. dist. (Å)	C−Br···(Cl/S) (deg)	Br···(Cl/S)−C (deg)
Br1E···Cl1[b]	3.3098(7)	3.61	3.32	168.7(2)	91.4(8)
Br1B···S5[c]	3.446(4)	3.59	3.57	165.2(2)	117.4(3)
Br2B···S4	3.427(3)	3.59	3.57	176.4(2)	120.8(2)

[a] vdW dist. stands for van der Waals contact distance while anis. dist. stands for anisotropic contact distance defined as ($r_{\min\ Br} + r_{\max\ Cl/S}$) with anisotropic radii taken from Nyburg and Faerman[29] (see also Scheme 2). [b] $1 + x, y, 1 + z$. [c] $1 - x, 1 - y, -z$.

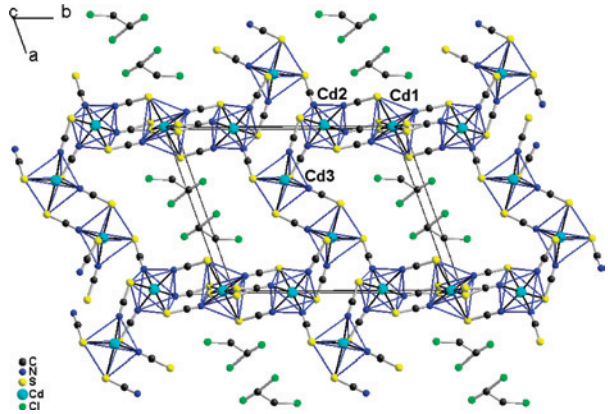

Figure 5. Solid-state organization of the anionic network in **2**, showing the Cd octahedra associated into Cd2−Cd1−Cd2 trimers, linked together with penta-coordinated cadmium (Cd3) complexes located at the center of the unit cell.

bidentate ligands (Figure 5). As a consequence, Cd1 and Cd2 are hexacoordinated, and these octahedra form trimeric Cd2−Cd1−Cd2 entities aligned along *b*, strongly reminiscent of the chains observed in the structure of the starting electrolyte, [Et$_4$N][Cd(SCN)$_3$] with three NCS$^-$ ligands linking the octahedra. These trimers are linked together by pentacoordinated Cd3 complexes located at the center of the unit cell. This structural organization leaves large empty spaces within the anion layer which are filled by two inversion-centered 1,1,2-trichloroethane molecules.

The Complex Organic Conducting Layers. Let us now concentrate on the organic slabs in **1** and **2** and the

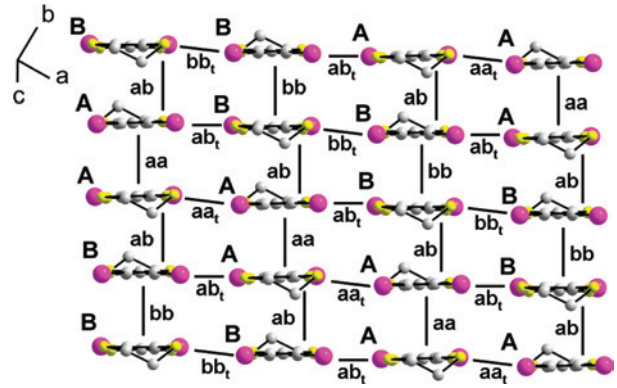

Figure 6. Solid-state organization within the organic slabs in **1**. Absolute values of the β_{ij} interaction energies (see text): for the *intrastack* interactions, $\beta_{aa} = 0.374$ eV, $\beta_{bb} = 0.397$ eV, and $\beta_{ab} = 0.333$ eV; for the interstack interactions, $\beta_{aat} = 0.084$ eV, $\beta_{bbt} = 0.081$ eV, and $\beta_{abt} = 0.103$ eV.

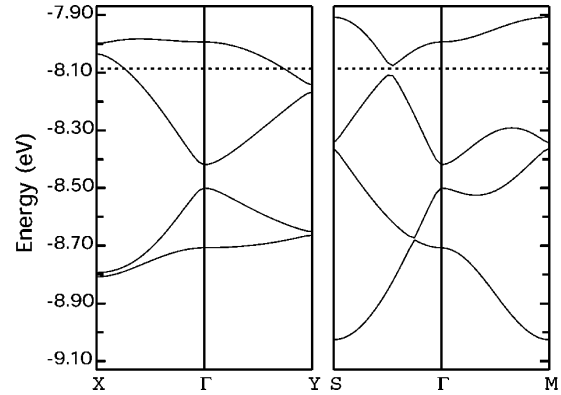

Figure 7. Extended Hückel calculated band structure of **1**, $\Gamma = (0, 0)$, $X = (a^*/2, 0)$, $Y = (0, b^*/2)$, $M = (a^*/2, b^*/2)$, $S = (-a^*/2, b^*/2)$. The dotted line indicates the Fermi level according to the stoichiometry, for metallic behavior.

relationship between their structural organization and the conducting properties of the two salts. As shown in Figure 6 for salt **1**, we observe that the partially oxidized EDT-TTF-I$_2$ donor molecules organize into chains running along $a-b$, with inversion-centered head-to-tail A−A bimolecular motifs, alternating with B−B motifs. These −A−A−B−B− chains interact laterally along $a + b$ with neighboring stacks with essentially in-registry types of interactions. The three AA, BB, and AB overlaps within the chains are of the bond-over-ring type, allowing us to describe these phases as β phases.[31]

HOMO−HOMO overlap interaction energies (β_{ij}) between two neighboring molecules within the organic slab were determined by tight-binding extended Hückel calculations[32] (see Figure 6 caption). The strongest interactions are essentially limited to the stacks running along $a-b$, while lateral interactions between stacks are about 4 times smaller. This lets us anticipate a sizable one-dimensional character for this salt. Band structure calculations (Figure 7) show indeed a large dispersion for the bands running along the

(31) Mori, T. *Bull. Chem. Soc. Jpn.* **1998**, *71*, 2509.
(32) Since overlap is explicitly included in extended Hückel calculations, these interaction energies (β) should not be confused with the conventional transfer integrals (t). Although the two quantities are obviously related and have the same physical meaning, the absolute values of β are somewhat larger than those of t.

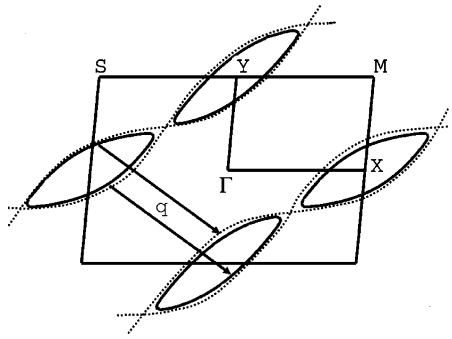

Figure 8. Calculated Fermi surface for **1**, showing closed loops around the *X* and *Y* points, Γ = (0, 0), *X* = (*a**/2, 0), *Y* = (0, *b**/2), *M* = (*a**/2, *b**/2), *S* = (−*a**/2, *b**/2). The dotted lines show the pseudo one-dimensional nature of this structure, with the associate *q* vector (1/2, −1/2) allowing for perfect nesting of this reconstructed 1D surface.

stacks (Γ → *S*), but a more limited one in the perpendicular interstack direction (Γ → *M*). Despite the fact that we are in the presence of the semiconductor and not a metal, and considering the $\rho = 0.5$ charge transfer degree determined from the stoichiometry of the salt, the calculated Fermi level value does not cut any band along the Γ → *M* or Γ → *S* directions, but along Γ → *X* or Γ → *Y*. The corresponding Fermi surface for this stoichiometry (Figure 8) shows the presence of closed loops around the *X* and *Y* points of the Brillouin zone, which would indicate a two-dimensional electronic structure, in contradiction with our former analysis of the different β_{ij} values for the intra- and interstack interactions. However, a closer inspection shows that this motif can be rebuilt from the superposition of two quasi 1D open surfaces (shown in dotted lines in Figure 8), confirming the 1D character of this salt. Furthermore, we also observe that the two dotted lines are efficiently nested by a reciprocal vector $q = (1/2, -1/2)$, a hidden nesting[33] which can be at the origin of the semiconducting behavior of the salt.

Salt **2** crystallizes (Figure 9) with five crystallographically independent EDT-TTF-Br_2 molecules (A−E), which associate into −ABCED−ABCED− stacks running along (*a*−*b*), with the neighboring stacks generated by the inversion centers located between the stacks. Differences between the central C═C bond lengths among the five crystallographically independent molecules are observed, ranging indeed from 1.356(8) to 1.387(8) Å, and indicating a possibility for a degree of charge localization.[9b] Note also that one of the EDT-TTFBr_2 molecules (molecule C) was found disordered on two positions (Figure 10) with a 73:27 distribution determined from the crystal structure refinement of the two positions. Such a strong disorder of halogenated TTFs is relatively frequent within chlorinated TTFs[5] but has been already encountered once in a monoiodo EDT-TTF-I salt.[12a] In the following, we will therefore restrict our calculations of HOMO···HOMO interaction energies (β_{ij}) and band structure to the situation encompassing the major isomer of molecule C. The calculated β_{ij} values (see Figure 9 caption)

(33) (a) Whangbo, M. H.; Canadell, E.; Foury, P.; Pouget, J.-P. *Science* **1991**, *252*, 96. (b) Whangbo, M. H.; Ren, J.; Liang, W.; Canadell, E.; Pouget, J. P.; Ravy, S.; Williams, J. M.; Beno, M. A. *Inorg. Chem.* **1992**, *31*, 4169. (c) Martin, J. D.; Doublet, M. L.; Canadell, E. *J. Phys.* **1993**, *3*, 2451.

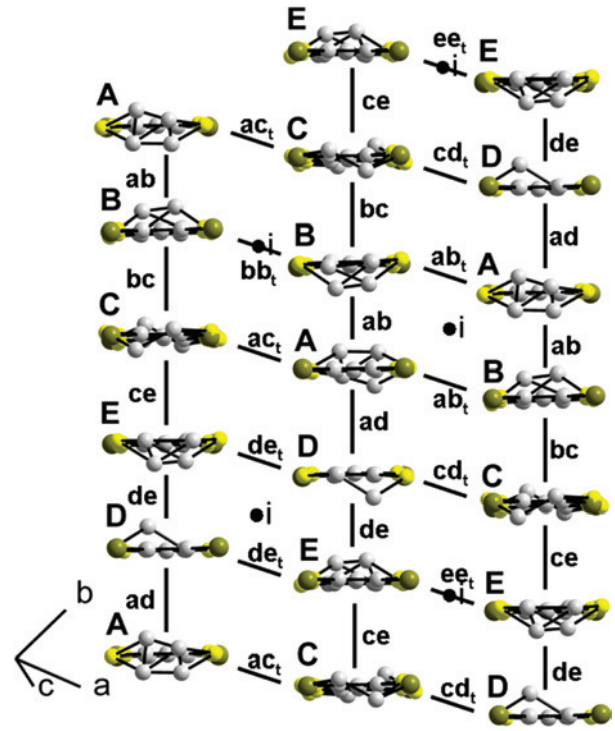

Figure 9. Solid-state organization within the organic slabs in **2**. The inversion centers are indicated as (•i). Absolute values of the β_{ij} interaction energies (see text): for the *intrastack* interactions, $\beta_{ab} = 0.377$ eV, $\beta_{bc} = 0.380$ eV, $\beta_{ce} = 0.364$ eV, $\beta_{ad} = 0.408$ eV, and $\beta_{de} = 0.393$ eV; for the *interstack* interactions, $\beta_{abt} = 0.049$ eV, $\beta_{cdt} = 0.064$ eV, $\beta_{eet} = 0.059$ eV, $\beta_{det} = 0.047$ eV, $\beta_{act} = 0.032$ eV, and $\beta_{bbt} = 0.034$ eV.

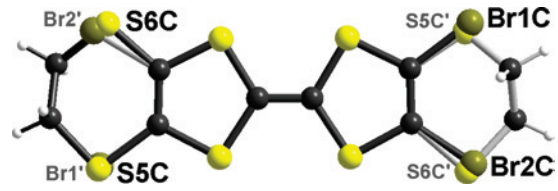

Figure 10. Disorder model adopted by the EDT-TTF-Br_2 molecule C in **2**. The major orientation (73.4%) is shown with dark bonds, the minor one (26.6%) with light gray bonds.

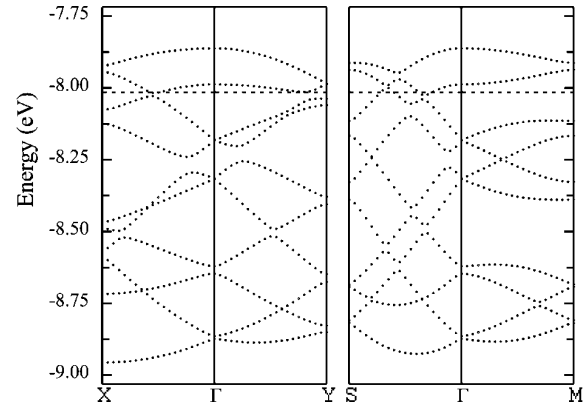

Figure 11. Calculated band structure for **2**, Γ = (0, 0), *X* = (*a**/2, 0), *Y* = (0, *b**/2), *M* = (*a**/2, *b**/2), *S* = (−*a**/2, *b**/2). The dotted line indicates the Fermi level according to the $\rho = +0.4$ oxidation level.

are 6−7 times larger in the stacking direction than in the perpendicular ones, a situation which lets us infer a stronger one-dimensional character for this salt than for **1**.

Band structure calculations for salt **2** (Figure 11) show a strong dispersion of the 10 bands in the Γ → *S* direction

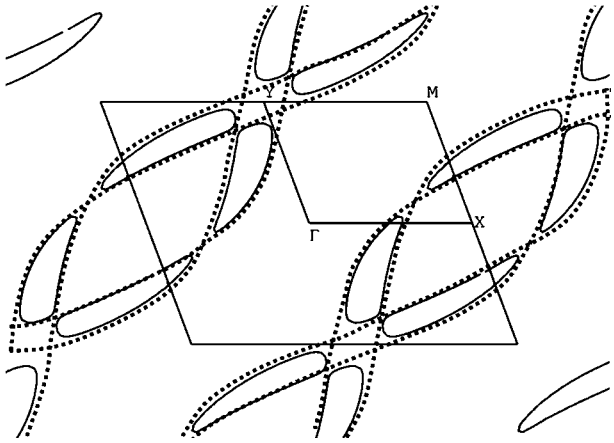

Figure 12. Calculated Fermi surface for **2**. Γ = (0, 0), $X = (a^*/2, 0)$, $Y = (0, b^*/2)$, $M = (a^*/2, b^*/2)$, $S = (-a^*/2, b^*/2)$. The dotted lines show the hidden one-dimensional nature of this electronic structure.

associated with the stacking of the EDT-TTF-Br_2 molecules along $(-a + b)$, while these dispersions are indeed much smaller in the perpendicular direction ($\Gamma \rightarrow M$). Considering the $\rho = +0.4$ charge transfer deduced from the stoichiometry of the salt, the two upper bands should be empty. However, the calculated Fermi level cuts several bands, affording a calculated Fermi surface (Figure 12) with closed pockets.

As already noticed for salt **1**, this 2D character is only apparent. The dotted lines represented in Figure 12 shows indeed the hidden one-dimensional nature of the salt, which was already anticipated from the large intrastack interaction energies, when compared with the interstack ones. The comparable corrugation of these surfaces most probably allows for several efficient nesting processes which will destroy the possible metallic character of the salt.

The Relationships between Anionic and Organic Layers. The difference in the degree of charge transfer between the two salts can be related to the ratio between the average anionic charge per surface unit in both compounds and the effective area occupied by one donor molecule within the 2D conduction layer. Such an approach has been recently developed by Kato et al. in their investigations of three-component conducting salts[34] where the introduction of increasingly larger neutral molecules in the anionic layer was shown to stabilize unusual oxidation states of the donor molecules, an important issue in the search for deliberate setting of the incommensurate band fillings in molecular metals.[28] Similarly, a series of salts of 2,5-bis(1,3-dithiol-2-ylidene)-1,3,4,6-tetrathiapentalene (BDT-TTP) with one single β-type conducting layer was associated with isosteric rhenium cluster anions of increasing charge (from −1 to −4), allowing for the investigation of an extended set of negative charge densities of the inorganic template unit frame.[35] In BEDT-TTF salts with 2D layer structures, one BEDT-TTF molecule is known to occupy about 25−30 Å^2

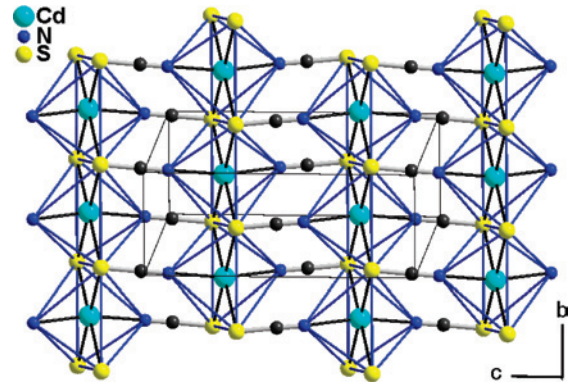

Figure 13. The two-dimensional polymeric network adopted by the anionic $[Cd_2(SCN)_6]^{2-}$ species in α-$[BEDT\text{-}TTF]_3[Cd_2(SCN)_6]$.[36]

within the conduction layer. In the present salts, we observe that the EDT-$TTFI_2$ molecule in **1** occupies 28.3 Å^2 while, as anticipated, the dibromo derivative occupies a smaller 24.3 Å^2 surface in **2**. On the other hand, a more compact anionic layer is found in **1** with one negative charge spread over 57 Å^2, while it is spread over 61 Å^2 in **2**. Both effects combine here to afford an exact 2:1 stoichiometry in **1**, while a larger number of the smaller EDT-$TTFBr_2$ molecules are needed to cover the larger surface of the anionic layer incorporating the TCE molecules, hence the smaller ($\rho = 0.4$) and unconventional degree of charge transfer in **2**, with its associated higher conductivity.

These complex structural organizations also indicate a strong reorganization of the 1D motifs of the starting electrolyte, with, in both salts, a default of the SCN^- anion when compared with the starting $[Cd(SCN)_3]^-$ stoichiometry. In **1**, the SCN-deficient $[Cd_3(NCS)_8]^{2-}$ motif is completed by a water molecule, while in **2**, the $[Cd_5(SCN)_{14}]^{4-}$ motif is not compensated and one out of the three Cd ions is only pentacoordinated. This behavior contrasts with the only reported TTF salt in the cadmium thiocyanate series, that is, α-$[BEDT\text{-}TTF]_3[Cd_2(SCN)_6]$, where the $[Cd(SCN)_3]^-$ stoichiometry was maintained in the final product.[36] This salt was obtained directly from $Cd(SCN)_2$, NH_4SCN, and 18-crown-6 in a TCE/EtOH mixture. The chainlike motif of the alkyl ammonium salts was not observed, but as shown in Figure 13, it was a two-dimensional compact array with every Cd^{2+} in an octahedral environment. We observe however that, in **2**, the 1D motif of the starting electrolyte is not completely lost since linear trimeric Cd2−Cd1−Cd2 entities (Figure 5) have been excised out of the starting $[Cd(SCN)_3]_\infty^-$ infinite chains. The main difference in the elaboration of the salts described here and the BEDT-TTF salt relies on the Cd/SCN ratio used as an electrolyte. In our case, a strict 1:3 ratio was used, while in the BEDT-TTF salt, an excess of SCN^- anions was used. This observation indicates a possible experimental way to modify the final stoichiometry and band filling by performing those electrocrystallizations with various Cd/SCN ratios.

(34) (a) Yamamoto, H. M.; Yamaura, J.-I.; Kato, R. *J. Am. Chem. Soc.* **1998**, *120*, 5905. (b) Yamamoto, H. M.; Kato, R. *Bull. Chem. Soc. Jpn.* **2006**, *79*, 1148. (c) Yamamoto, H. M.; Kato, R. *Chem. Lett.* **2000**, 970.

(35) Perruchas, S.; Boubekeur, K.; Canadell, E.; Misaki, Y.; Auban-Senzier, P.; Pasquier, C.; Batail, P. *J. Am. Chem. Soc.* **2008**, *130*, 3335.

(36) Mori, H.; Tanaka, S.; Mori, T.; Maruyama, Y. *Bull. Chem. Soc. Jpn.* **1995**, *68*, 1136.

Conclusions

We have shown here that the polymeric $[Cd(SCN)_3]^-_\infty$ anion undergoes, under electrocrystallization conditions, a complete reorganization, probably based on an autofragmentation/rearrangement process.[37] This ability of polymeric inorganic networks to reorganize in solution is related to the concept of mere excision in solution of monomeric molecular motifs from low-dimensional inorganic solids.[38] Compared with the regular $[Cd(SCN)_3]$ stoichiometry, which allows for a complete Cd^{2+} hexacoordination and the formation of chains or layers, the thiocyanate deficiency in the $[Cd_3(NCS)_8]^{2-}$ and $[Cd_5(SCN)_{14}]^{4-}$ motifs observed here is stabilized through water coordination or pentacoordination, allowing for the formation of hollow layers with solvent inclusion. The acetonitrile molecule in **1** is anchored to the organic network through a linear C−I···NC−CH_3 halogen interaction involving one iodine atom of the EDT-$TTFI_2$ molecules, while a larger cavity in **2** allows for the incorporation of two 1,1,2-trichloroethane molecules, with one chorine atom bonded to one of the partially oxidized EDT-$TTFBr_2$ molecules through a characteristic C−Br···Cl−C halogen interaction with C−Br···Cl and Br···Cl−C angles close to 180 and 90°, respectively. In both salts, halogen bonding to the sulfur atoms of the SCN anion is also observed, despite its involvement in Cd^{2+} coordination.

Because of this inclusion of the larger TCE molecules, the anionic charge per surface unit is decreased in **2** when compared with **1**. Combined with the smaller effective area occupied by one EDT-$TTFBr_2$ molecule within the 2D conduction layer, it affords in **2** an unusual stoichiometry with nonconventional charge transfer ($\rho = 0.4$), associated with a notably higher conductivity. Band structure calculations and Fermi surface analysis in both salts would indicate two-dimensional electronic behavior associated with the presence of electron and hole pockets. We have shown however that these closed Fermi surfaces could be reconstructed from pseudo-1D Fermi surfaces with a strong corrugation, but allowing for an efficient hidden nesting.

Acknowledgment. We thank Thierry Roisnel (CDIFX, Rennes, France) for the X-ray data collections. Financial support of the Agence Nationale de la Recherche (ANR contract CHIRASYM no. NT05-2 42710) is gratefully acknowledged.

Supporting Information Available: A CIF file of reported complexes. This material is available free of charge via the Internet at http://pubs.acs.org.

IC801207V

(37) Sayettat, J.; Bull, L. M.; Gabriel, J.-C. P.; Jobic, S.; Camerel, F.; Marie, A.-M. M.; Fourmigué, M.; Batail, P.; Brec, R.; Inglebert, R.-L. *Angew. Chem., Int. Ed. Engl.* **1998**, *37*, 1711.

(38) (a) Feliz, M.; Guillamon, E.; Llusar, R.; Vicent, C.; Stiriba, S.-E.; Perez-Prieto, J.; Barberis, M. *Chem.—Eur. J.* **2006**, *12*, 1486. (b) Yaghi, O. M.; Scott, M. J.; Holm, R. H. *Inorg. Chem.* **1992**, *31*, 4778. (c) Long, J. R.; Williamson, A. S.; Holm, R. H. *Angew. Chem., Int. Ed. Engl.* **1995**, *34*, 226. (d) Jin, S.; DiSalvo, F. J. *Chem. Mater.* **2002**, *14*, 3448. (e) Lee, S. C.; Holm, R. H. *Angew. Chem., Int. Ed. Engl.* **1990**, *29*, 840.